MUST Journal of Research and Development (MJRD) Volume 6 Issue 3, September 2025
e ISSN 2683-6467 & p ISSN 2683-6475

Dye Sorption from Textile Wastewater onto Faujasite Zeolite Synthesized from Bauxite Sediment and Rice Husk Silica

[1]Frederick O. Oshomogho[*], [2]Felix Omoruwou, [3]Doris Ngozi Onwenna and [4]Osariemen Edokpayi

[1,4] Department of Chemical Engineering, University of Benin, PMB1154, Benin City, Edo State

[2] Department of Chemical Engineering, Federal University of Petroleum Resources, PMB 1221, Effurun, Delta State

[3] Department of Chemical Engineering, University of Delta, Agbor PMB 2090, Agbor, Delta State

DOI: https://doi.org/10.62277/mjrd2025v6i30012

ARTICLE INFORMATION

Article History

Received: 22nd June 2025
Revised: 24th August 2025
Accepted: 06th August 2025
Published: 30th September 2025

Keywords

Clay
BET
Isotherm
Fixed-bed
Breakthrough curve

ABSTRACT

This study explores the adsorptive properties of high silica-containing zeolite synthesised from natural sediments rich in aluminosilicates, modified with biowaste silica for wastewater treatment. Hydrothermal synthesis was used to produce zeolite from local clay sediment. The synthesised zeolite was tested for its ability to adsorb ionic dyes from textile wastewater. XRD and EDS analysis revealed a faujasite zeolite-Y with 85.60 g of Si and 17.50 g of Al, and a Si/Al ratio of 4.891 g/mol. The Zeolite Y particles had a uniform size distribution ranging from 1 to 3 µm. The Langmuir isotherm analysis showed a specific surface area of 1,750 m^2/g and a pore diameter of 1.847 nm. Batch adsorption experiments yielded Langmuir, Freundlich, and Temkin regression constants with R^2 values below 0.9924, 0.9451, and 0.9395, respectively, during an isothermal study on methylene blue sorption. The fixed-bed column test indicated an adsorbent stability of 5.25 hours. Overall, the faujasite zeolite-Y, with its large mesoporous structure, demonstrates significant adsorption of ionic dye from textile effluent.

*Corresponding author's e-mail address: fred.oshomogho@uniben.edu (Oshomogho, F.O)

1.0 Introduction

Zeolites are crystalline minerals composed of hydrated aluminosilicates. They consist of tetrahedral units of silicon and aluminium atoms, which are connected by sharing their oxygen atoms. This arrangement creates regular cavities and channels within the crystal, which have very small diameters. The hydrothermal process has been used in the preparation of zeolite from natural deposits containing silica, alumina, cations, and water. Different types of silica-containing sources, such as kaolin clay, are naturally occurring in Nigeria (Oyedoh et al., 2023). It is known that various kinds of silica can yield different kinds of zeolites from the identical gel combination. In the production of zeolite, the majority of silica sources are readily accessible as solutions, gels, fumed solids, colloids, and organic variants such as tetra-ethyl-orthosilicate (Mamudu et al., 2020). Other sources of silica, such as silica-bearing plants, can also be used to synthesise zeolite.

Zeolite has been applied in a wide range of industrial applications, including the substitution of the hazardous phosphate builder in detergent manufacture. Zeolite can be used as a catalyst in the petroleum and hydrocarbon industries to enhance the effectiveness of chemical reactions, conserving energy and thereby reducing pollution (Mamudu et al., 2020). Low-silica zeolites, such as zeolite Na-A and zeolite Na-X, are widely used in a variety of technological applications, including ion exchange, adsorption, and catalysis, as well as the treatment of radioactive wastewater, sewage effluent, agricultural wastewater, fluid catalytic cracking, and other processes (Li & Pidko, 2019). Consequently, there is an ongoing search for both raw materials to be used in the synthesis processes of these materials and for the economic optimisation of synthesis protocols.

Textile wastewater contains various contaminants, primarily characterised by high levels of COD, BOD, dissolved solids, and colour pigments. During the dyeing process, a significant amount of dye remains unfixed on the fabric and is discharged directly into water bodies. Most textile dyes are resistant to photodegradation, oxidation, and biodegradation. If textile wastewater is not properly treated, it can pose serious environmental risks. Coloured water is visually unappealing, and the dyes prevent sunlight from penetrating the water, which inhibits photosynthesis and harms aquatic life (Rahman et al., 2017).

This study explored the development of a highly stable faujasite zeolite adsorbent for wastewater treatment containing methylene blue. The synthesis of a catalyst from local sediments and agricultural waste with adsorption capabilities aims to provide a cheap and effective way to treat polluted wastewater from local industries. Silica and alumina are among the most common mineral components on earth and are the primary raw materials needed to synthesise zeolite; therefore, the supply of zeolite is virtually unlimited.

2.0 Materials and Methods

The chemicals and reagents used in this research were purchased from various internationally certified producers as well as local analytical chemical dealers.

2.1 Synthesis of Zeolite from Extracted Alumina and Rice Husk Silica

An adequate volume of standard NaOH solution was prepared and gradually added to a specific mass of alumina and rice husk silica mixture to form an aluminosilicate gel. The gel was continuously stirred at room temperature for 120 minutes using a magnetic stirrer and allowed to age for 24 hours. A hydrothermal treatment was then performed on the mixture at 120°C for approximately 6 hours in an autoclave. Afterward, the mixture was washed with deionised water until reaching a neutral pH. The washed sample was dried in an oven for about 4 hours at 105°C to remove moisture. The dried sample was cooled to ambient temperature in a desiccator and subsequently analysed to determine the type of zeolite formed.

2.2 Application of Zeolite in Adsorption

A batch adsorption experiment was conducted using about 100 ml of the simulated effluent containing various concentrations of pollutants. Different dosages of 0.1 to 1.50 g of the zeolite were weighed into a 250 ml conical flask and placed on an orbital shaker with a shaking speed set at a constant 140 rpm. In each experimental condition, the sample was withdrawn and filtered with Whatman's filter paper, and the filtrate was analysed for the percent dye adsorbed.

2.3 Batch Adsorption Experimental

Different dosages of zeolite were varied from 0.1 to 1.5g/100ml (1.0 to 15g/l) and placed into five 200 ml bottles containing 100 ml of effluent at ambient temperature. To study the impact of contact times of zeolite on the effluent, the adsorption time ranged from 10 to 60 minutes, with the adsorbent concentration set at approximately 10g/L.

The samples will be agitated for about 60 minutes with an orbital shaker, filtered, and then analysed. The percentage of pigment removal, *Pr*, was computed by Eq. 1 according to (Navya et al., 2020):

$$P_r = \frac{(C_0 - C_i)}{C_0} \times 100 \quad (1)$$

Also, the dye uptake, q (mg/g) by zeolite was determined with Eq. (1)

$$q = \frac{(C_o - C_f) * V}{m} \quad (2)$$

Where C_o and C_f are the initial and final dye concentration in mg/l, respectively, V is the volume of effluent in litres, and m is the adsorbent dose in grams.

2.4 Batch Adsorption Isotherm Study

Employing the Langmuir, Freundlich, and Temkin isotherm models, adsorption equilibrium data for the solid in the solution system were analysed. It was discovered that these constants expressed the adsorbent's affinity and surface features.

2.4.1 Langmuir Isotherm

The Langmuir isotherm is predicated on the notion that there is a monolayer of adsorbate molecules on the adsorbent surface and that all adsorption sites are identical and have the same energy. For homogeneous adsorption, the Langmuir adsorption isotherm model (Eqn 3) is typically utilised, and it has proven to be effective in monomolecular adsorption processes. Equation 4 illustrates how the Langmuir model is presented in linear form.

$$\frac{C_e}{q_e} = \frac{1}{q_m b} + \frac{C_e}{q_m} \quad (4)$$

where,

Ce, the dye's equilibrium constant, is given in mg/L. The amount of dye adsorbed at equilibrium, qe, is given in mg/g. Two associated concepts are the Langmuir constant, Qm, and the energy of the adsorption capacity, L/mg. The Figure will display the Ce/qe linear plot against Ce. The values of the constants qm and b can be computed using the plot's slope and intercept, and the results are displayed in the table below. To identify high-affinity adsorption, the dimensionless constant separation term (RL) was used to examine the Langmuir isotherm's structure.

Irreversible (R_L=0), favourable (0< R_L<1), linear (R_L = 1), or unfavourable (R_L > 1) isotherms are all indicated by R_L. R_L was calculated as follows:

$$R_L = \frac{1}{1 + bC_o} \quad (5)$$

Where C_0 is the initial dye concentration (mg/L).

2.4.2 Freundlich Isotherm

assumes that the adsorption process is not limited to a single layer of adsorbate molecules and that a variety of energies are present at the adsorption sites (Udeagbara et al., 2021). The Freundlich isotherm model can be used to assess the adsorption intensity of the adsorbate on the adsorbent surface. The linear form of the Freundlich model is represented by:

$$log q_e = log k_f + \frac{1}{n} log C_e \quad (7)$$

where n is the Freundlich factor of the Freundlich isotherm constant associated with adsorption intensity, kf is the Freundlich isotherm constant associated with adsorption capacity (L/mg), and qe and Ce are the dye concentrations in solid and solution, respectively, at equilibrium (mg/g and mg/L). The values of n and kf are determined using the slope and intercept of the log qe vs. log Ce linear plot. The 1/n numbers show whether the isotherm is irreversible (1/n = 0), unfavourable (1/n > 1), or advantageous (0 < 1/n < 1).

2.4.3 Temkin Isotherm

A consistent distribution of binding energies throughout the group of surface binding adsorption was predicted using the Temkin isotherm model. The Temkin isotherm model was used to predict a uniform distribution of binding energies over the population of surface binding adsorption (Oladoja *et al.* 2008). The linear form of the Temkin equation was expressed as shown (Equation 8).

$$q_e = \beta \ln \alpha + \beta \ln C_e \quad (8)$$

where, $\beta = \frac{RT}{b}$ (9)

The Temkin constant (b), which is equivalent to the heat of sorption (J/mg), the universal gas constant (R), 8.314 J/mol K, and the absolute temperature in Kelvin are all provided. Plotting qe against lnCe will yield the isotherm constants α and b; the parameters are displayed in the table below.

2.5 Adsorption in a Fixed Bed Column

Laboratory column experiments were conducted isothermally in a 500cm-long, 40mm-diameter glass column at (29±2)℃. A 35.62g modified faujasite zeolite sample was filled to a height of H = 20 cm in the column. Zeolite bulk density, ρ, was 0.699 g/cm^3, and fixed bed porosity, β, was 69.3%. The funnel with a valve circulated the feeding solution, a 100 mg/L methylene blue solution, through the bed

in down-flow mode at a flow rate of Q = 2.5 cm^3/min throughout the process. The bed depth, temperature, pressure, and flow rate were all maintained at consistent levels to prevent the material in the columns from contracting or expanding. Using a UV-Vis Spectrophotometer, the experiment's effluent samples were routinely taken, and their methylene blue levels were measured.

2.5.1 Modelling of Breakthrough Curves

For an adsorption column, the Thomas model expression is provided as in Eqn 10, according to (Kumari & Dey, 2019)

$$ln\left(\frac{C_o}{C_t}-1\right)=\left(\frac{k_{Th}q_o m}{Q}\right)-k_{Th}C_o t \qquad (10)$$

where q_o is the equilibrium level of dye uptake per g of the adsorbent (mg/g), kTh is the Thomas rate constant (ml/(min mg)), Ct is the effluent dye content for time (mg/l), m is the mass of the adsorbent in the column (g), and Q is the flow rate (ml/min).

The ratio of influent and effluent dye concentrations is represented by the value of Ct/Co. Breakthrough time is represented by the value of t (min, t = Veff /Q, where Veff is the effluent solution volume). Since the values of C_t/C_o fall between 0.05 and 0.95, nonlinear regression analysis can be used to predict the values of k_{Th} and q_o from a plot of C_t/C_o aganst t. The plot of $ln\left[\left({}^{C_o}/_{C}\right)-1\right]$ vs. t at a specific flow rate can be used to calculate the kinetic coefficient kTh and the bed's adsorption capacity q0.

3.0 Results and Discussion

3.1 Results of BET Analysis of Synthesized Zeolite

The synthesized zeolite has a BET specific surface area of 1750.0 m2/g, as determined by the Langmuir isotherm study. The pore width, measured using the HK technique, is approximately 1.847 nm. The crystallinity of the material can be inferred from its microscopic appearance. The adsorption capacity of an adsorbent increases with its surface area. The micropore volume of the synthesized zeolite is calculated to be 485.4 cc/g, and the total pore volume is 881.0 cc/g, according to the HK and DFT methods. The surface area, determined by the multi-point BET plot, is 287.252 m2/g, while the average pore diameter, measured via the DA technique, is 214 nm. Using the BJH method, the pore diameter is 3.108 nm, the pore volume is 0.140 cc/g, and the surface area is 290.370 m2/g. The materials display pore sizes within the mesoporous range. The H3 hysteresis loop indicates slit-like platelets. Narrow hysteresis loops were observed, and the N2 uptake capacity was similar at P/Po values near 1. The materials showed microporosity at low relative pressures. At higher P/Po values, the curve of the synthesized zeolite continued upward, indicating macroporosity.

3.2 Results of EDS Analysis of Modified Faujasite Zeolite

The Si/Al ratio in the improved zeolite catalyst was measured using an energy-dispersive X-ray spectrometer. Figure 2 displays the ratio of 4.891, which was the result of the presence of Si at 85.60wt% and Al at 17.50wt%. This zeolite is a faujasite, and zeolite Y often has a Si/Al ratio greater than 2 (Eletta et al., 2018). An increase in the Si/Al ratio improves zeolite stability (García-Martínez et al., 2012; Mgbemere et al., 2019).

Figure 2

EDS Spectrum of Modified Faujasite Zeolite

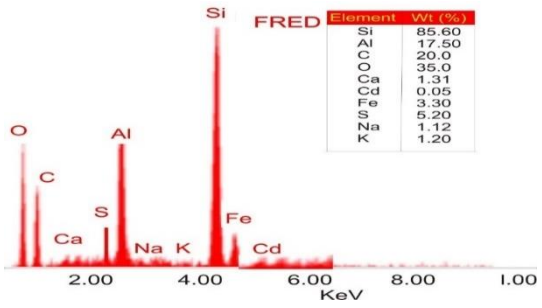

3.3 Results of SEM of Synthesized Zeolite

SEM images of zeolite at various magnifications revealed a clear particle with a fuzzy disk-like 2D particle form (Figure 3). The microscopy demonstrated that the zeolite has particle morphologies and meets the American Petroleum Institute requirement for molecular sieves in general. The peak at 565 cm^{-1} is caused by the zeolite-specific double-ring external bond. External linkage symmetrical stretching is responsible for the peak at 685 cm^{-1}, whereas internal tetrahedral symmetrical stretching is responsible for the peak at 775 cm^{-1}. The peaks at 1010 cm^{-1} and 1080 cm^{-1} represent the stretching of the interior tetrahedral asymmetry and the outer linkage asymmetry, respectively.

It could also be owing to the presence of unused Na impurities in the mother liquor (Novembre et al., 2011).

Figure 3

(a) SEM Micrograph of Synthesized Faujasite Zeolite at two Magnifications of (a) 9000x and (b) 8000x

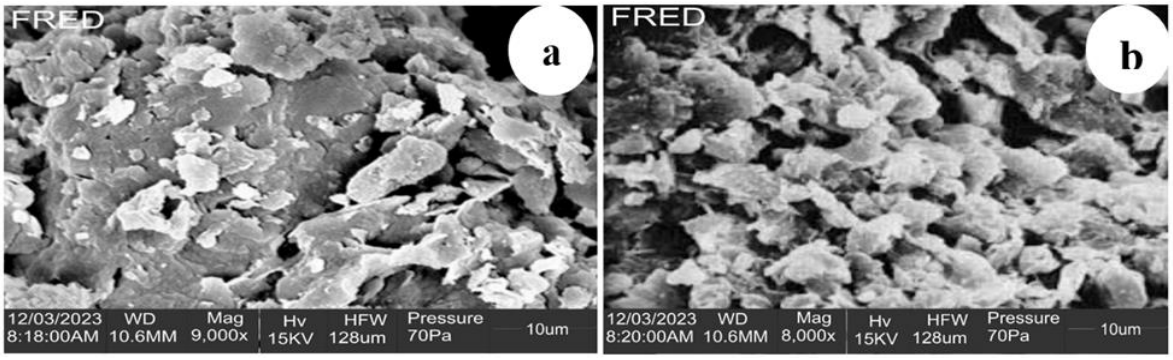

3.4. Adsorption Property of Synthesized Zeolite on Textile Effluent

Figures 4 to 6 show the results of the adsorption capacity of zeolite on textile effluent containing methylene blue as an ionic dye pigment. Figure 4 shows that the percentage of dye removed by the zeolite increased as the contact time increased from 10 minutes to 60 minutes. The dye removal efficiency increased steadily from 50% at 10 minutes to over 90% at 60 minutes. This indicates that a longer contact time allows for more adsorption of the dye onto the zeolite surface. The effect of different zeolite dosages on dye removal efficiency was further illustrated in Figure 5, which revealed a notable rise in removal % as the dosage rose from 1.0 g/L to 10.0 g/L. Overall, the findings point to zeolite as a successful adsorbent for eliminating methylene blue from textile wastewater.

Figure 4

Effect of Adsorption Time on Dye Removal by Synthesized Zeolite At 3g/L Adsorbent Dosage and 300mg/L of Dye Concentration

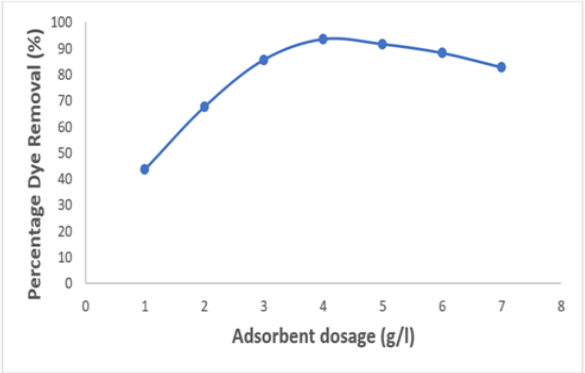

Figure 5

Effect of Adsorbent Dosage on Dye Pigment Removal by Synthesized Zeolite at 30 Minutes of Adsorption and 300mg/L Dye Concentration

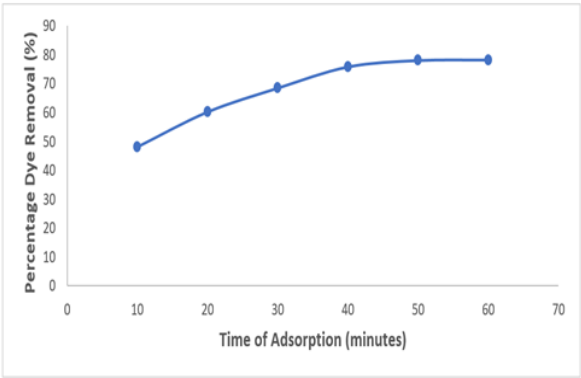

The findings demonstrated that as resident duration increases, so does the percentage reduction of methylene blue over time at a constant adsorbent dosage of 3g/l of effluent, with time ranging from 10 to 60 minutes. According to Figure 5's profiles, the removal efficiency rose quickly and then tended to remain constant after roughly 50 minutes of equilibrium. It is demonstrated that the quantity of zeolite present affects the adsorption of dye pigment (Figure 5). It was discovered that the effective removal rate of methylene blue first rose with an increase in the amount of adsorbent utilised, reaching a maximum of 93.49% in terms of the percentage of dye removed, before starting to decline. The adsorbent dose of 4.0 g/l produced the highest possible absorption, while 1.0 g/l produced the lowest possible uptake.

Figure 6

Effects of Initial Dye Concentration on Percentage Dye Removal

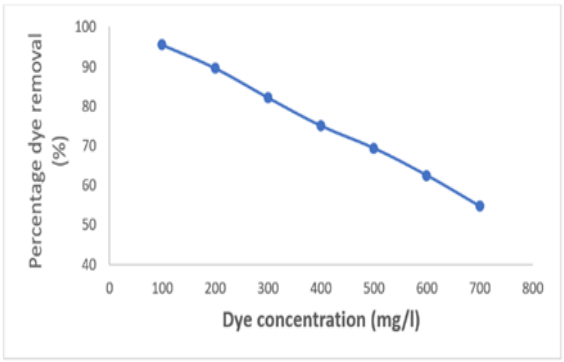

3.5 Adsorption Isotherms

The equilibrium isotherms were generated by varying the temperature and determining the material's adsorption capacity at each temperature. The study presented the adsorption capacities at five different adsorbent doses, ranging from 1.0g/L to 5.0g/L. The results indicate a higher affinity between the material and the adsorbate at higher concentrations since the adsorption capacity grows in tandem with the adsorbent's dose.

3.5.1 Langmuir Isotherms

Langmuir isotherms are valid for monolayer adsorption onto a surface containing a finite number of identical sites (Udeagbara et al., 2021). Due to its excellent agreement with sorption experimental data, this model is the most often utilised. As shown in Figure 7, a plot of (Ce⁄qe) vs. Ce was made to identify the constants, qm and kL, in the Langmuir isotherm. The plot's vertical axis intercept was $1/k_{Lqm}$, and its slope was 1/qm. The experimental data were then correlated using these constants. The regression coefficient, R^2 was 0.9924 and was closest to unity. This experimental data can be used to correlate the equilibrium data.

Figure 7

Langmuir Adsorption Isotherm Plot

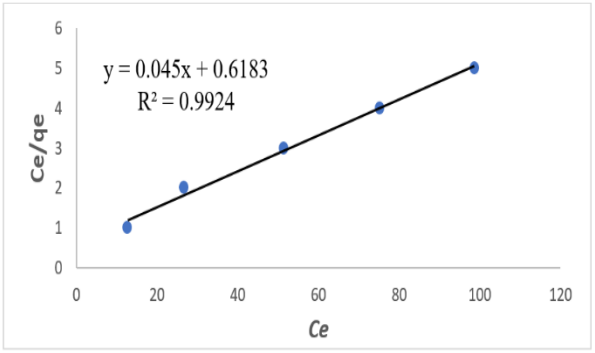

3.5.2 Freundlich Isotherm

The Freundlich isotherm theory (Awokoya et al., 2016) described the amount of methylene blue adsorbed per gram of zeolite (*qe*). It may be applied to adsorption onto heterogeneous surfaces and is the most often utilised method. The Freundlich isotherm is shown as *In q* vs. *In Ce* in Figure 8; having a slope of (1/n) and an intercept on the vertical axis of (*In kf*) allows for the determination of the constants n and kf. If the Freundlich isotherm correlates with the experimental data, n should be greater than unity. It was observed that the batch adsorption data could be correlated by the linear isotherm since a straight line was obtained, with intercepts on both horizontal and vertical axes for the linear isotherm. Since n = 4.2301, which is greater than 1, estimated from the straight line obtained using the Freundlich isotherm plot shown in Figure 4.30, then the Freundlich isotherm can also be used to correlate the equilibrium data with the regression coefficient, R^2, being 0.9451, which is very close to unity. The other constant in the Freundlich isotherm was found to be kf = 6.648.

Figure 8

Freundlich Adsorption Isotherm Plot

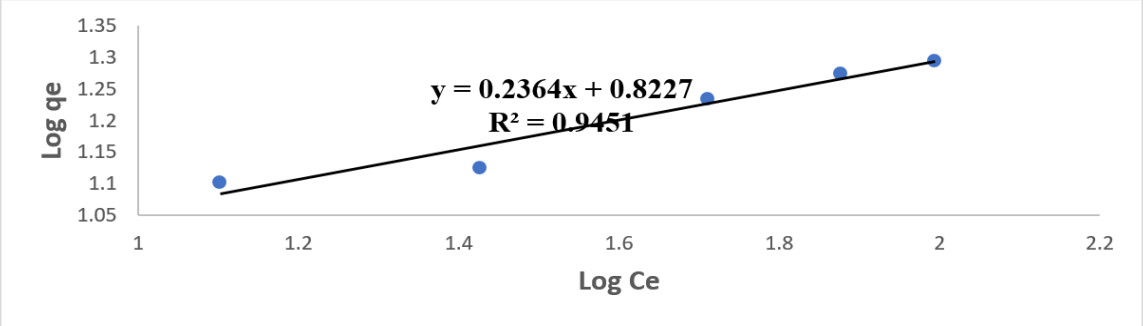

3.5.3 Temkin Isotherm

The Temkin isotherm model was used to estimate a consistent distribution of binding forces throughout the surface contact adsorption species (Oladoja et al., 2008). The Temkin isotherm study results are shown in Figure 9. The results revealed the regression value R^2 = 0.9395. This made this model the least fitted to describe the data obtained.

Figure 9

Temkin Adsorption Isotherm Plot

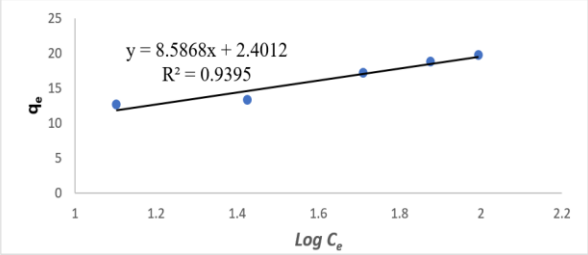

For the Freundlich, Langmuir, and Temkin constant's results. The Langmuir isotherm with R^2 < 0.9924, the Freundlich isotherm with R^2 < 0.9451, and the Temkin isotherm with R^2 < 0.9395 showed the poorest match; hence, no additional analysis of these models was pursued. These models effectively capture the adsorption behaviour of the system being studied. The R-squared values of 0.9924, 0.9451, and 0.9395 for Langmuir, Freundlich, and Temkin isotherms indicate a strong correlation between the experimental and projected values based on these models.

3.6 Fix Bed Adsorption Study: Breakthrough Curve Analysis

From Figure 10, C_t/C_o as a function of time was used to represent Methylene Blue loading from a fixed-bed solution (Akbar et al., 2020). Assessing the elimination of Methylene Blue dye using modified Faujasite zeolite adsorbent by analysing the C_t/C_o ratio over time during adsorption. C_t/C_o reached 99.05% to determine the breakthrough and saturation times.

Figure 10

The Breakthrough Curve

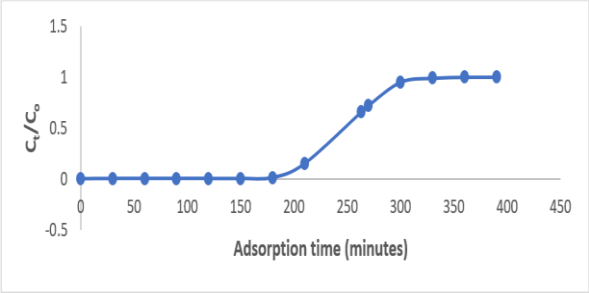

3.6.1 Break Time Analysis

The breakthrough curve (BTC) theory was examined in a fixed-bed column to assess the performance of the synthesized zeolite. The operation of the adsorption column and its dynamic response depend on the BTC breakthrough time and shape. The concentration-time profile of the BTC influences the adsorption dynamics and process design. Figure 10 shows the normalised dye concentration (Ct/Co) plotted against time (min) for BTC at a constant flow rate. The BTC results indicated that a breakthrough occurred at 180 minutes, marking the point where the adsorbent's stability began to decline. This may be due to increased adsorption in areas with a steady flow rate of the substance being absorbed, which reduces the time needed to reach the designated breakthrough concentration. The fraction of total capacity that broke through at 63.4% demonstrated that the synthesized zeolite adsorbent performed well in removing the ionic dye from the solution, as evidenced by the stability (tt) of 5.25 hours.

Table 1

Parameters Obtained from BTC of the Fixed-Bed Column for MB Removal by Synthesized Faujasite Zeolite

Parameter	Unit	Value
Adsorbent stability time (t_t)	*hr*	5.25
Breakthrough point time (t_u)	*hr*	3.33
Fraction of total capacity to break through	%	63.40
Height of used bed (H_T)	cm	20.00
Length of used bed (H_B)	cm	12.69
Unused bed (H_{UNB})	cm	7.32
Influent flow rate (Q)	mg/h	3420
Sorbate adsorbed	mg	13125
Adsorbent saturation capacity (q_e)	$mg_{mb}/g_{zeolite}$	368.47

Table 1 shows that column 368.47 mg/g zeolite had an adsorption capacity of 13125 mg and a dye removal % at a steady flow rate before reaching the breakpoint. The adsorbent's surface characteristics, dye structures, and experimental conditions all had an impact on the adsorption capacity. Several studies observed a similar kind of observation in diverse systems (Eberle et al., 2023; Halalsheh et al., 2022); as a result, flow time influences the retention period of dye molecules in the column and influences the adsorbent-dye contact time. In general, Table 4.3 shows that the packed-bed column performs better when it comes to removing methylene blue.

3.6.2 The Thomas Models

The Thomas rate constant (k_{Th}) and maximum solid phase concentration were determined by analysing the breakthrough behaviour of MB using the Thomas model (Figure 11). Relative constants were computed using a non-linear regression approach. The significant correlation between Ct/Co and t is indicated by the R^2 value of 0.9654. Since the concentration difference between the dye on the adsorbent surface and the dye in the solution is the main driving element for adsorption, an influent concentration of 100 mg/l affects both the qo value and the k_{Th} value. The initial adsorption capacity (q_0) and Thomas rate constant (k_{Th}) were ascertained by nonlinear regression analysis. With an R^2 value of 0.9654, the regression coefficients analysis demonstrated that the regressed patterns fit the experimental data well. This resulted in k_{TH} of 0.00056 ml/min.mg and q0 of 17510.923 mg/g.

Figure 11
The Thomas Model Plot

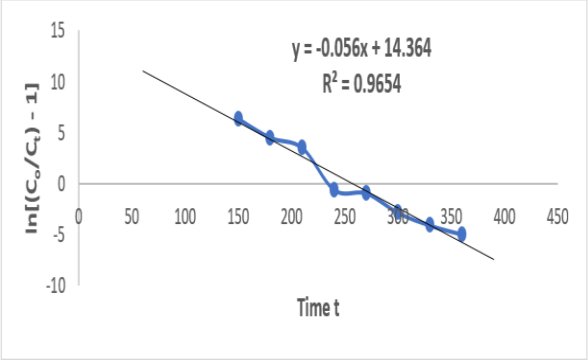

4.0 Conclusion

The study examined zeolite synthesis, characterisation from local clay sediments and its use as a catalyst for adsorbing ionic dye pigments in textile wastewater. High-purity alumina (82.11 wt%) and silica (77.449 wt%) can be extracted from local clay sediments, which can be used to synthesize zeolite with a higher silicon-to-aluminium molar ratio of approximately 4.891. Infrared spectra analysis detected a zeolite framework structure, and additional confirmation from EDXRF, BET, and SEM-EDS indicated that a Faujasite-type zeolite-Y was produced. The batch adsorption study showed that the Langmuir model best describes the uptake of methylene blue by nanoporous Faujasite zeolite, with an R^2 of 0.9924. A fixed-bed adsorption test demonstrated that the Faujasite zeolite catalyst has high adsorption capacity for treating textile wastewater containing ionic dyes, maintaining stability for over 5 hours in a fixed bed.

5.0 Acknowledgements

The authors hereby acknowledge the management of Luco Chemical Laboratory for providing the workbench and analytical equipment for conducting the experimental analysis.

6.0 References

Akbar, N. A., Rosman, N. D., Hambali, S., & Abu Bakar, A. A. (2020). Adsorption of methylene blue by banana stem adsorbent in a continuous fixed bed column study. *IOP Conference Series: Earth and Environmental Science*, *616* (1).https://doi.org/10.1088/1755-1315/616/1/012058

Awokoya, K., Sanusi, R., Oninla, V., & Ajibade, O. (2016). Activated Periwinkle Shells for the Binding and Recognition of Heavy Metal Ions from Aqueous Media. *International Research Journal of Pure and Applied Chemistry*, *13*(4), 1–10. https://doi.org/10.9734/irjpac/2016/31440

Ayoub, M., Ullah, S., Inayat, A., Bhat, A. H., & Hailegiorgis, S. M. (2016). Process Optimization for Biodiesel Production from Waste Frying Oil over Montmorillonite Clay K-30. *Procedia Engineering*, *148*, 742–749. https://doi.org/10.1016/j.proeng.2016.06.60

6

Eberle, S., Schmalz, V., Börnick, H., & Stolte, S. (2023). Natural Zeolites for the Sorption of Ammonium: Breakthrough Curve Evaluation and Modeling. *Molecules*, *28*(4). https://doi.org/10.3390/molecules28041614

Eletta, O., Mustapha, S. I., Ajayi, O., & Ahmed, A. T. (2018). *Optimization of Dye Removal from Textile Wastewater using Activated Carbon from Sawdust*. *March*. https://doi.org/10.4314/njtd.v15i1.5

García-Martínez, J., Li, K., & Krishnaiah, G. (2012). A mesostructured Y zeolite as a superior FCC catalyst – from lab to refinery. *Chemical Communications*, *48*(97), 11841–11843. https://doi.org/10.1039/c2cc35659g

Halalsheh, N., Alshboul, O., Shehadeh, A., Al Mamlook, R. E., Al-Othman, A., Tawalbeh, M., Saeed Almuflih, A., & Papelis, C. (2022). Breakthrough Curves Prediction of Selenite Adsorption on Chemically Modified Zeolite Using Boosted Decision Tree Algorithms for Water Treatment Applications. *Water (Switzerland)*, *14*(16), 2519. https://doi.org/10.3390/w14162519

Kumari, R., & Dey, S. (2019). A breakthrough column study for the removal of malachite green using coco-peat. *International Journal of Phytoremediation*, *21*(12), 1263–1271. https://doi.org/10.1080/15226514.2019.1633252

Li, G., & Pidko, E. A. (2019). The Nature and Catalytic Function of Cation Sites in Zeolites: a Computational Perspective. *ChemCatChem*, *11*(1), 134-156. https://doi.org/10.1002/cctc.201801493

Mamudu, A., Emetere, M., Okocha, D., Taiwo, S., Ishola, F., Elehinafe, F., & Okoro, E. (2020). Parametric investigation of indigenous Nigerian mineral clay (Kaolin and Bentonite) as a filler in the Fluid Catalytic Cracking Unit (FCCU) of a petroleum refinery. *Alexandria Engineering Journal*, *59*(6), 5207–5217. https://doi.org/10.1016/j.aej.2020.09.050

Mgbemere, H. E., Ekpe, I. C., Lawal, G., Ovri, H., & Chaudhary, A. L. (2019). Preparation and characterization of zeolite type 4a using kaolin from Ajebo, Nigeria. *Pertanika Journal of Science and Technology*, *27*(4), 2427–2438.

Navya, A., Nandhini, S., Sivamani, S., Vasu, G., Sivarajasekar, N., & Hosseini-Bandegharaei, A. (2020). Preparation and characterization of cassava stem biochar for mixed reactive dyes removal from simulated effluent. *Desalination and Water Treatment*, *189*, 440–451. https://doi.org/10.5004/dwt.2020.25635

Novembre, D., di Sabatino, B., Gimeno, D., & Pace, C. (2011). Synthesis and characterization of Na-X, Na-A and Na-P zeolites and hydroxysodalite from metakaolinite. *Clay Minerals*, *46* (3), 339-354. https://doi.org/10.1180/claymin.2011.046.3.339

Oladoja, N. A., Asia, I. O., Aboluwoye, C. O., Oladimeji, Y. B., & Ashogbon, A. O. (2008). Studies on the sorption of basic dye by rubber (Hevea brasiliensis) seed shell. *Turkish Journal of Engineering and Environmental Sciences*, *32*(3), 143–152.

Oyedoh, EA; Okwah, GA; Oshomogho, F. (2023). Physicochemical Characteristics of Clay Mineral from Ikpeshi in Akoko-Edo Local Government Area , Edo State , Nigeria. *J. Appl. Sci. Environ. Manage. March*, *27*, 1119–1125. https://doi.org/: https://dx.doi.org/10.4314/jasem.v27i6.9

Rahman, M., Ahmed, T., Salehin, I., & Hossain, M. (2017). Color removal from textile wastewater using date seeds activated carbon. *Bangladesh Journal of Scientific and Industrial Research*, *52*(1), 31-42. https://doi.org/10.3329/bjsir.v52i1.32083

Udeagbara, S., Isehunwa, S., Okereke, N.U., & Kerunwa, A. (2021). Management of Produced Water from Niger-Delta Oil Fields Using a Local Material. *Journal of Petroleum and Environmental Biotechnology*, *12*(10), 351.